

Numerical Simulations of Intermittent Transport in Scrape-Off Layer Plasmas

O. E. Garcia, V. Naulin, A. H. Nielsen, and J. Juul Rasmussen

Association EURATOM-Risø National Laboratory,

OFD-128 Risø, DK-4000 Roskilde, Denmark

(Dated: July 16, 2018)

Abstract

Two-dimensional fluid simulations of interchange turbulence for geometry and parameters relevant for the scrape-off layer of confined plasmas are presented. We observe bursty ejection of particles and heat from the bulk plasma in the form of blobs. These structures propagate far into the scrape-off layer where they are lost due to transport along open magnetic field lines. From single-point recordings it is shown that the blobs have asymmetric conditional wave forms and lead to positively skewed and flat probability distribution functions. The radial propagation velocity may reach one tenth of the sound speed. These results are in excellent agreement with recent experimental measurements.

PACS numbers: 52.25.Gj, 52.35.Ra, 52.65.Kj

Recently, several experimental investigations have revealed a strongly intermittent nature of particle and heat transport in the scrape-off layer (SOL) of magnetized plasmas [1, 2, 3]. There are strong indications that this is caused by localized structures in the form of plasma “blobs” propagating radially far into the SOL. It has been suggested that this is due to the dipolar vorticity field caused by vertical guiding center motions in plasmas in non-uniform magnetic fields [4], reflecting the compressibility of the diamagnetic current. An outstanding challenge is to give a self-consistent description of the emergence and evolution of such structures, which also capture their statistical properties. Here an attempt towards this goal is presented, yielding favorable agreement with experimental measurements. This is achieved by focusing on the collective two-dimensional dynamics perpendicular to the magnetic field while using a simplified description of particle and heat losses to limiters or end plates along open field lines.

Some of the most prominent features of experimental single-point measurements are the presence of asymmetric conditional wave forms as well as strongly skewed and flat probability distribution functions (PDF’s) of the density and temperature signals [1, 2, 3]. Simple interpretations as well as advanced imaging techniques give a picture of field-aligned blobs or filaments propagating out of the bulk plasma with radial velocities up to one tenth of the sound speed. These highly non-linear thermal structures have amplitudes which significantly exceed the back-ground levels. The associated intermittent transport may have severe consequences for magnetic confinement experiments by producing large heat bursts on plasma facing components. A change of sign in the asymmetry of the fluctuation time series PDF close to the last closed flux surface (LCFS) indicates that the structures are generated by a “flapping” of the edge pressure gradient, ejecting blobs of excess particles and heat out of the bulk plasma [1]. The blob structures thus seems to be generated close to the LCFS and subsequently propagate far into the SOL, where they are subject to strong damping due to parallel losses. This separation of driving and damping regions in configuration space has been discarded in several previous studies of SOL turbulence [5, 6].

In this Letter we present a novel model for interchange turbulence in slab geometry and numerical solutions in qualitative agreement with experimental measurements. The model geometry comprises distinct production and loss regions, corresponding to the edge and SOL of magnetized plasmas. The separation of these two regions defines an effective LCFS, though we do not include magnetic shear in our model. In the edge region, strong pressure gradients maintain a state of turbulent convection. It is demonstrated that a self-regulation mechanism involving differential rotation leads to a repetitive expulsion of hot plasma into the SOL, resulting in asymmetric con-

ditional wave forms, strongly non-Gaussian probability distributions and significant cross-field transport by localized objects.

Assuming cold ions and neglecting electron inertia effects, a three-field model may be derived for quasi-neutral electrostatic perturbations of the full particle density n , electric potential ϕ and electron temperature T . Using the Bohm normalization and slab coordinates with $\hat{\mathbf{z}}$ along the magnetic field we obtain [7],

$$\begin{aligned} \left(\frac{\partial}{\partial t} + \hat{\mathbf{z}} \times \nabla \phi \cdot \nabla \right) \Omega - C(p) &= \nu_{\Omega} \nabla^2 \Omega - \sigma_{\Omega} \Omega, \\ \frac{dn}{dt} + nC(\phi) - C(nT) &= \nu_n \nabla^2 n - \sigma_n (n - 1) + S_n, \\ \frac{dT}{dt} + \frac{2T}{3} C(\phi) - \frac{7T}{3} C(T) - \frac{2T^2}{3n} C(n) &= \nu_T \nabla^2 T - \sigma_T (T - 1) + S_T, \end{aligned}$$

where time is normalized by the ion gyration period, $1/\omega_{ci}$, and spatial scales by the hybrid gyration radius, $\rho_s = c_s/\omega_{ci}$. The particle density n and temperature T are normalized to fixed characteristic values at the outer wall. We further define the two-dimensional advective derivative, the magnetic field curvature operator and the toroidal magnetic field, respectively, by

$$\frac{d}{dt} = \frac{\partial}{\partial t} + \frac{1}{B} \hat{\mathbf{z}} \times \nabla \phi \cdot \nabla, \quad C = -\zeta \frac{\partial}{\partial y}, \quad B = \frac{1}{1 + \varepsilon + \zeta x}.$$

The vorticity is given by $\Omega = \nabla_{\perp}^2 \phi$, the inverse aspect ratio $\varepsilon = a/R_0$ and $\zeta = \rho_s/R_0$ where a and R_0 are the minor and major radius of the device, respectively. The terms on the right hand side of the model equations describe external sources S , parallel losses along open field lines through the damping rates σ , and collisional diffusion with coefficients ν . The geometry and boundary conditions are sketched in Fig. 1.

In the absence of external forcing and dissipative processes the model equations non-linearly conserves the global energy

$$E = \int d\mathbf{x} \left[\frac{1}{2} (\nabla_{\perp} \phi)^2 + \frac{3}{2} nT \right],$$

where the integral extends over the whole plasma layer under consideration. Thus, the curvature terms due to magnetic field inhomogeneity correctly yield a conservative energy transfer from the confined heat to the convective motions. We further define the kinetic energy of the fluctuating and mean components of the flows,

$$K = \int d\mathbf{x} \frac{1}{2} (\nabla_{\perp} \tilde{\phi})^2, \quad U = \int d\mathbf{x} \frac{1}{2} v_0^2, \quad (1)$$

where the zero index denotes an average over the periodic direction y and the spatial fluctuation about this mean is indicated by a tilde. The linearly damped mean flows, $v_0 = \partial\phi_0/\partial x$, does not yield any radial convective transport and hence form a benign path for fluctuation energy. The energy transfer rates from thermal energy to the fluctuating motions, and from the fluctuating to the mean flows, are given respectively by

$$F_p = \int d\mathbf{x} n T C(\phi), \quad F_v = \int d\mathbf{x} \tilde{v}_x \tilde{v}_y \frac{\partial v_0}{\partial x}. \quad (2)$$

Note that F_p is essentially a measure of the domain integrated convective thermal energy transport, while F_v shows that structures tilted such as to transport positive poloidal momentum up the gradient of a sheared flow will sustain the flow against collisional dissipation [8, 9, 10].

In the following we present results from numerical simulations of the interchange model using parameters relevant for SOL plasmas. The dimensions of the simulation domain is $L_x = 2L_y = 400$ and the LCFS is located at $x_{\text{LCFS}} = 100$. The parameters used for the simulation presented here are $\varepsilon = 0.25$, $\zeta = 10^{-3}$, and the collisional diffusion $\nu = 5 \times 10^{-3}$ is taken to be the same for all fields. The parallel loss rate of temperature is assumed to be five times stronger than that on the density and vorticity, $\sigma_n = \sigma_\Omega = \sigma_T/5 = 10^{-3}/2\pi q$, since primarily hot electrons are lost through the end sheaths [11]. The damping rates σ_n and σ_Ω correspond to losses along one connection length $2\pi R_0 q$ with the acoustic speed c_s , where $q = 3$ is the safety factor at the edge. Finally, the radial line-integral of the sources S_n and S_T equals 0.2, and the shape of the sources and parallel loss coefficients shown in Fig. 1 are given by $\delta = 16$ and $\xi = 2$. For the numerical solution we have employed an Arakawa scheme for the advective non-linearities and a third order stiffly stable scheme for the time integration [7]. The spatial resolution is 512 and 256 grid points in the radial and poloidal directions, respectively, and the total time span of the simulation is 4×10^6 .

In Fig. 2 we show the typical evolution of the particle confinement P and heat confinement H in the edge and SOL regions, defined by

$$P_{\text{edge}} = \int_0^{x_{\text{LCFS}}} dx n_0(x, t), \quad P_{\text{SOL}} = \int_{x_{\text{LCFS}}}^{L_x} dx n_0(x, t),$$

and similarly for the heat confinement H . From the figure we observe that plasma and heat gradually builds up in the edge at the same time as it is decaying in the SOL region. This is repetitively interrupted by rapid changes in which plasma and heat is lost from the edge to the SOL. More than 20% of the edge plasma may be lost during individual bursts. Also note from the figure that the normalized heat confinement is much less than the particle confinement due to the larger loss rate

in the SOL region of the former. Further insight is revealed by Fig. 3 which shows the evolution of the kinetic energy contained by the mean and fluctuating motions, confer Eq. (1), as well as the collective energy transfer terms defined in Eq. (2). From the figure we observe that the convective energy and thermal transport appears as bursts during which particles and heat are lost from the edge into the SOL region. As discussed in Refs. 8, 9, 10, this global dynamics is caused by a self-regulation mechanism in which kinetic energy is transferred from the fluctuating to the mean components of the flows, and subsequently damped by collisional dissipation. As the thermal confinement is allowed to vary, this results in characteristic sawtooth oscillations [8]. Note, however, the clear demonstration in Figs. 2 and 3 that thermal energy is ejected in a bursty manner from the edge and into the SOL region, where it is eventually lost by transport along open field lines.

The time-averaged profiles of the plasma density and the mean poloidal flows are shown in Fig. 4. Parallel losses in the SOL region result in average profiles peaked inside the LCFS, and weakly decaying throughout the SOL. Also shown in Fig. 4 are typical instantaneous profiles during a quiet period (t_{quiet}) and during a burst (t_{burst}). We observe significant deviations from the average profiles, with a more peaked density profile in the edge region during quiet phases. During bursts there is a substantial increase of the density profile in the SOL region due to the convective plasma transport. The temperature profiles have a similar structure but with lower amplitudes due to the larger loss rate. The self-sustained poloidal flow profiles are strongly sheared in the edge region, and have larger amplitudes during the the strong fluctuation period. This figure clearly indicates that fluctuations are driven in the strong pressure gradients in the edge region.

The statistics of single-point recordings at different radial positions P_i indicated in Fig. 1 completely agree with experimental measurements. In Fig. 5 we present the probability distribution functions of the density signals taken from a long-run simulation containing more than a hundred burst events. The flat and strongly skewed distributions indicate the high probability of large positive fluctuations corresponding to blobs of excess plasma. The skewness and flatness factors take values up to 3 and 15, respectively, except for the outermost radial position (P_7) where very few structures arrive. At the other points the PDF's have similar structure with a pronounced exponential tail towards large values, a characteristic feature of turbulent convection in the presence of sheared flows [8, 9].

The conditionally averaged temporal wave forms calculated from the same signals, using the trigger condition $n > 4n_{\text{rms}}$ at each individual point, are presented in Fig. 6. An asymmetric wave form with a sharp rise and a relatively slow decay, as observed in experimental measurements, is

clearly seen [1, 2, 3]. The maximum density excursions significantly exceed the background level, and decay rapidly as the structures propagate through the SOL. The number of realizations for the conditional averaging decreases gradually from 125 at the innermost probe to 2 at the outermost one. Using a negative amplitude for the conditional averaging results in very few realizations, again showing the presence of blob-like structures. From two-dimensional animations and simple statistical correlation measurements we further find that the radial propagation velocity of these structures is typically about one tenth of the sound speed but with a large statistical variance. This is in excellent agreement with experimental measurements [1, 2, 3].

In Fig. 7 we show the spatial structure of the density, temperature, vorticity and electrostatic potential during a quiet period and during a burst. These correspond to the same times as the instantaneous profiles shown in Fig. 4. In the quiet period there are only weak spatial fluctuations with the plasma and heat well confined within the LCFS. During bursts we observe strong structures in all fields, which have propagated far into the SOL. Notice again the much weaker perturbation in the temperature field as compared to the density due to the difference in the parallel loss rates. Moreover, while blob-like structures are observed for the density and temperature fields, the vorticity displays a roughly dipolar structure as expected from theory and experimentally measured [1, 4].

In this Letter we have proposed a new model for interchange turbulence and demonstrated that its numerical solutions are in good agreement with that reported from experimental investigations of SOL turbulence and transient transport events [1, 2, 3]. An important feature of our model is the spatial separation between forcing and damping regions which has not been accounted for in previous studies [5, 6]. While our model does not in detail describe the transition region between closed and open magnetic field lines, its solution clearly demonstrates a sound mechanism for the origin and nature of intermittent transport in the SOL of magnetized plasmas. Our work verifies the present experimental working hypothesis in terms of field-aligned blob-like structures propagating far into the scrape-off layer, which was recently questioned by Sarazin *et al.* [5]. The blob-like transport results in strongly skewed and flat PDF's and asymmetric conditional wave forms. This is caused by a "flapping" of the edge pressure profile, ejecting blobs of excess particles and heat out of the bulk plasma. The excellent qualitative agreement between simulation data and experimental observations gives strong confidence that the two-dimensional structure in potential, vorticity, density and temperature of the blobs reveals the actual spatial shape of these blobs as occurring in experiments.

This work was supported by the Danish Center for Scientific Computing through grants no. CPU-1101-08 and CPU-1002-17. O. E. Garcia has been supported by financial subvention from the Research Council of Norway.

-
- [1] J. A. Boedo *et al.*, J. Nucl. Mater. **313–316**, 813 (2003); Phys. Plasmas **10**, 1670 (2003); *ibid.* **8**, 4826 (2001) D. L. Rudakov *et al.*, Plasma Phys. Control. Fusion **44**, 717 (2002).
- [2] G. Y. Antar *et al.*, Phys. Plasmas **10**, 419 (2003); *ibid.* **8**, 1612 (2001); Phys. Rev. Lett. **87**, 065001 (2001).
- [3] J. L. Terry *et al.*, Phys. Plasmas **10**, 1739 (2003); S. J. Zweben *et al.*, *ibid.* **9**, 1981 (2002); R. J. Maqueda *et al.*, *ibid.* **8**, 931 (2001).
- [4] S. I. Krasheninnikov, Phys. Lett. A **283**, 368 (2001) D. A. D’Ippolito, J. R. Myra and S. I. Krasheninnikov, Phys. Plasmas **9**, 222 (2002); N. Bian, S. Benkadda, J.-V. Paulsen and O. E. Garcia, *ibid.* **10**, 671 (2003).
- [5] Y. Sarazin, Ph. Ghendrih, G. Attuel, C. Clément, X. Garbet, V. Grandgirard, M. Ottaviani, S. Benkadda, P. Beyer, N. Bian, C. Figarella, J. Nucl. Mater. **313–316**, 796 (2003); Y. Sarazin and Ph. Ghendrih, Phys. Plasmas **5**, 4214 (1998).
- [6] S. Benkadda, X. Garbet, and A. Verga, Contib. Plasma Phys. **34**, 247 (1994); O. Pogutse, W. Kerner, V. Gribkov, S. Bazdenkov, and M. Osipenko, Plasma Phys. Control. Fusion **36**, 1963 (1994).
- [7] A complete derivation of the model will be presented in an extended report of these results. See however V. Naulin, J. Nycander and J. Juul Rasmussen, Phys. Rev. Lett. **81**, 4148 (1998) and O. E. Garcia, J. Plasma Phys. **65**, 81 (2001).
- [8] O. E. Garcia, N. H. Bian, J.-V. Paulsen, S. Benkadda and K. Rypdal, Plasma Phys. Control. Fusion **45**, 919 (2003).
- [9] O. E. Garcia and N. H. Bian, “Bursting and large-scale intermittency in turbulent convection with differential rotation” accepted for publication in Phys. Rev. E (August 2003).
- [10] V. Naulin, J. Nycander and J. Juul Rasmussen, Phys. Plasmas **10**, 1075 (2003).
- [11] P. C. Stangeby, “The plasma boundary of magnetic fusion devices” (Bristol and Philadelphia: Institute of physics publishing, 2000).

FIG. 1: Geometry of the simulation domain showing the forcing region to the left, corresponding to the edge plasma, and the parallel loss region to the right, corresponding to the scrape-off layer. Data time series are collected at the probe positions P_i .

FIG. 2: Evolution of particle confinement P and the heat confinement H in the edge and scrape-off layer regions, showing sawtooth oscillations.

FIG. 3: Evolution of the kinetic energies and the collective energy transfer terms, showing bursty behavior in the fluctuation integrals.

FIG. 4: Time-averaged profiles of plasma particle density n_0 and mean poloidal flow v_0 , and typical profiles during a fluctuation burst and during a quite period.

FIG. 5: Probability distribution functions of density measured at seven different radial positions P_i as shown in Fig. 1. The vertical axis shows count numbers.

FIG. 6: Conditionally averaged wave forms of the density measured at seven different radial positions P_i as shown in Fig. 1, using the condition $n(x_{P_i}) > 4n_{\text{rms}}$.

FIG. 7: Typical spatial structure of density, temperature, vorticity and electric potential during a quite period to the left and during a burst to the right.

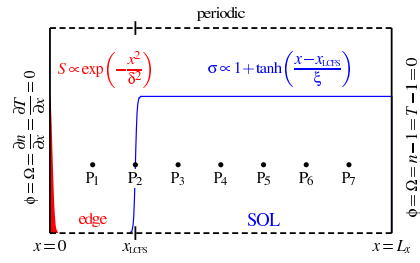


Figure 1

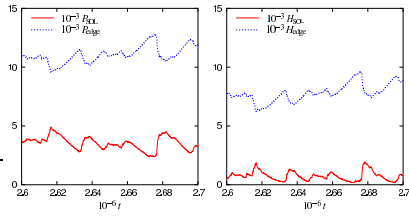


Figure 2

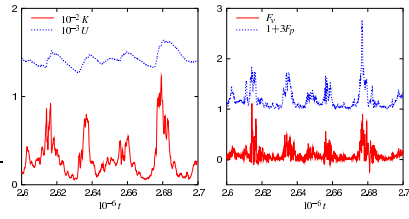


Figure 3

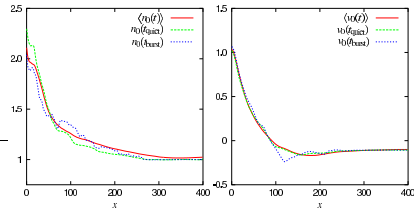


Figure 4

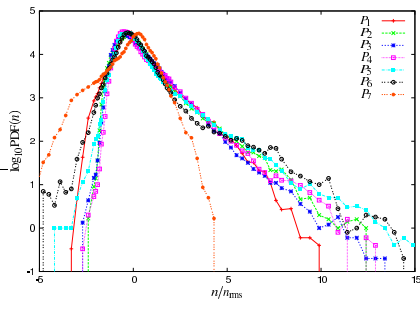


Figure 5

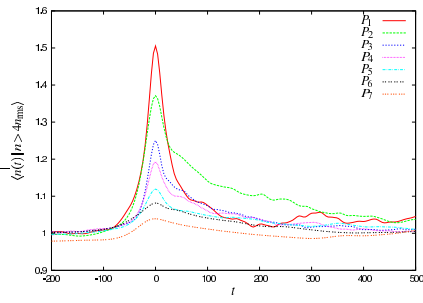


Figure 6

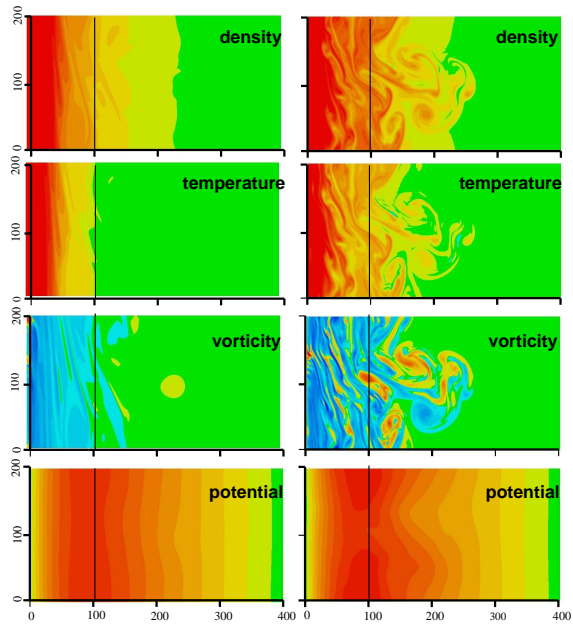


Figure 7